Sensorless Drive for Wound Rotor Synchronous Generator with Brushless Excitation System in Maritime DC Microgrid

Jonghun Yun[1], Sanggi Ko[2], Seung-Ki Sul[1], Woojae Park[2], Sanghyun Kim[2]
[1]Seoul National University, Republic of Korea
[2]Korea Shipbuilding and Offshore Engineering Co., Ltd., Republic of Korea

***Abstract*—The stator flux oriented control(SFOC) enables sensorless drive for a wound rotor synchronous generator (WRSG) in maritime dc microgrid. However, there have been few studies that considers the dynamics of the pilot exciter, which is used to indirectly control the field current of the main exciter. This paper proposes the SFOC considering the dynamics of the pilot exciter. The proposed SFOC finely tunes flux regulator based on the approximated model of the pilot exciter. Simulation and experimental tests were conducted with a 1.8 MW WRSG to verify the proposed SFOC.**

***Index Terms*—pilot exciter, sensorless drive, stator flux oriented control (SFOC), wound rotor synchronous generator (WRSG)**

I. Introduction

In pursuit of a sustainable and environmentally responsible shipping industry, electric propulsion systems have been progressed [1], [2]. Specifically, the DC power system stands out as one of promising technologies for electric vessels. Unlike its counterpart, AC power system, it enables variable engine speed operation. By adjusting the engine speed according to the load factor, the specific fuel cosumption can be minimized, resulting in enhanced engine efficiency, and reduced maintenance [3], [4].

For the construction of DC power systems, the wound rotor synchronous generator (WRSG) has generally been employed. Despite the superior dynamic performance and efficiency at light loads demonstrated by its counterpart, the permanent magnet synchronous generator (PMSG), the WRSG remains dominant in DC power systems due to its reliability and cost-effectiveness. As it has been extensively utilized not only in DC microgrids but also in AC microgrids for several decades, the WRSG benefits from a more well-established manufacturing infrastructure compared to the PMSG. Additionally, unlike the PMSG, which generates a field even in the idle state, the WRSG is capable of deactivating the excitation field, ensuring enhanced safety measures.

Although the excitation circuit in WRSG provides a degree of freedom to control the field, it can lead to a degradation in the efficiency and dynamic performance of the WRSG. The excitation current induces additional copper losses, and the dynamics of the excitation system need to be taken into consideration in order to regulate the field with the desired dynamic performance. To enhance the dynamic performance and efficiency of the WRSG, the utilization of an active-front-end (AFE) can be considered. In contrast to its counterpart, the diode-front-end (DFE), the AFE can regulate the current of the WRSG with less harmonic currents and achieve fast dynamic performance by actively adjusting the terminal voltage. Moreover, the AFE offers regeneration features, resulting in the rapid dynamics of DC bus voltage regulation.

For the DC bus voltage regulation of WRSG-AFE systems, stator flux -oriented control (SFOC), can be utilized, [5], [6], [7], [8]. The SFOC regulates the phase current on the reference frame synchronized to the stator flux while its counterpart, rotor flux-oriented control (RFOC), is performed on the reference frame synchronized to the rotor position. Compared to RFOC, SFOC offers advantages such as easier terminal voltage regulation and sensorless drive of WRSG. Under SFOC, the stator flux is aligned to the d-axis, allowing for the regulation of the stator flux magnitude by adjusting d-axis stator flux only. Estimation of stator flux can be performed without position sensor, resulting in cost reduction and enhanced reliability.

For field regulation under SFOC, the excitation current of the WRSG is adjusted. Typically, excitation in MW-scale WRSGs is carried out in two cascaded stages using a pilot exciter and a main exciter. This configuration enables brushless excitation and reduces the capacity of the field current regulator at the terminal. The pilot exciter indirectly produces the excitation current of the main exciter by rectifying the current of its rotating armature circuit. While the pilot exciter is commonly employed in MW-scale WRSGs, few studies have examined the dynamics of the pilot exciter under SFOC. To control WRSGs with faster dynamic performance, this paper proposes an SFOC approach that approximates the dynamics of the pilot exciter as a first-order system. Based on this approximation, the field regulation loop can be finely tuned to achieve the desired dynamic performance.

II. Proposed Stator Flux Oriented Control

Under SFOC, the power of the WRSG is expressed in terms of stator current at the q-axis, i^e_{qs}, and stator flux on the d-axis, λ^e_{ds}, as follows:

$$P_{gen} = -\frac{3}{2}\omega_e \lambda^e_{ds} i^e_{qs}. \tag{1}$$

In this equation, the subscript 'e' indicates the synchronous frame and ω_e represents the frequency, respectively. λ^e_{ds} is

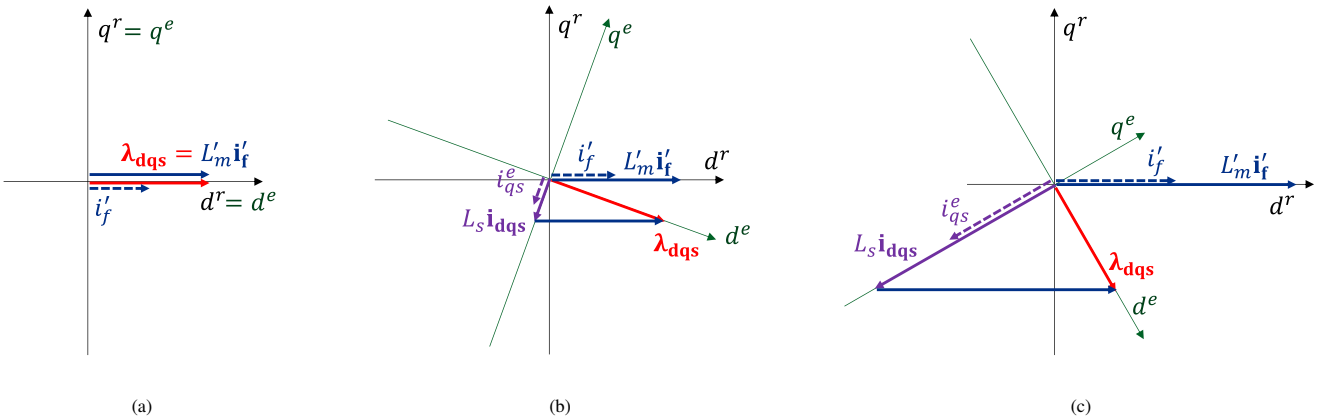

Fig. 1. Vector diagram for the SFOC under (a) no load condition, (b) light load condition, and (c) heavy load condition.

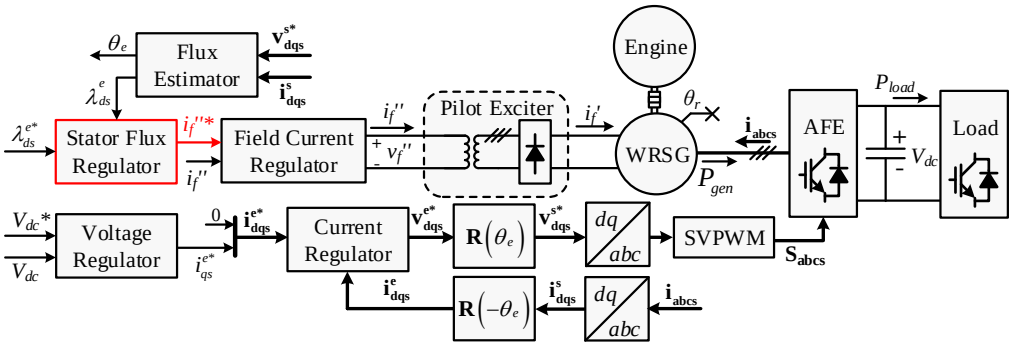

Fig. 2. Block diagram for the proposed SFOC for WRSG with a brushless excitation system.

regulated to constant value by adjusting the field current of the main exciter, i'_f.

Fig. 1 illustrates the adjustment of i'_f based on load conditions. As depicted in Fig. 1(b) and Fig. 1(c), an increase in load necessitates an increase in i'_f to maintain the magnitude of λ^e_{ds} due to the armature reaction of the increased i^e_{qs}. If i'_f increases slowly as the load increases, it can lead to AC under-voltage issues due to the weakening of i^e_{qs}. Conversely, if i'_f decreases slowly during load reduction, it may result in AC over-voltage problems. Therefore, achieving fast dynamics for the control of i'_f is crucial for stable AC voltage regulation of the WRSG. However, direct regulation of i'_f is not feasible within the brushless excitation system.

For enhancing the dynamics of the stator flux control loop with a brushless excitation system, this paper proposes an SFOC that takes into account the dynamics of the pilot exciter. The block diagram of the proposed SFOC is illustrated in Fig. 2. To regulate λ^e_{ds}, the field current of the main exciter, i'_f, needs to be controlled. Since direct regulation of i'_f is not possible, the field current of the pilot exciter, i''_f, is adjusted instead. Due to the difficulty in deriving a specific transfer function from the field current setpoint of the pilot exciter, i''^*_f, to λ^e_{ds}, this paper approximates the transfer function from i''^*_f to λ^e_{ds} as a first-order low-pass filter:

$$G_{ex}(s) = \frac{\lambda^e_{ds}(s)}{i''^*_f(s)} = \frac{i''_f(s)}{i''^*_f(s)}\frac{i'_f(s)}{i''_f(s)}\frac{\lambda^e_{ds}(s)}{i'_f(s)} \simeq k_{ex}\frac{\omega_{ex}}{s+\omega_{ex}}. \quad (2)$$

In this equation, the parameters, k_{ex}, ω_{ex}, can be extracted from the step response of the terminal voltage varying i''^*_f.

Based on the approximated model, the flux regulator can be designed using a PI regulator structure. To set the bandwidth of the flux regulator using ω_{fc}, the regulator can be designed as follows:

$$\begin{aligned} i''^*_f &= \left(k_p + \frac{k_i}{s}\right)\left(\lambda^{e*}_{ds} - \hat{\lambda}^e_{ds}\right), \\ k_p &= \frac{\omega_{fc}}{k_{ex}\omega_{ex}}, \quad k_i = \omega_{ex}k_p. \end{aligned} \quad (3)$$

With the proposed flux regulator, the transfer function of the stator flux regulation loop can be set with the desired bandwidth as:

$$\frac{\lambda^e_{ds}}{\lambda^{e*}_{ds}} \simeq \frac{\omega_{fc}}{s+\omega_{fc}}. \quad (4)$$

TABLE I. Parameters for test setup

Parameter	Value
Rated power of WRSG	1.8 MW
Rated voltage of WRSG	690 V
DC bus voltage	1100 V
Electrical frequency	60 Hz
Switching frequency	2.5 kHz

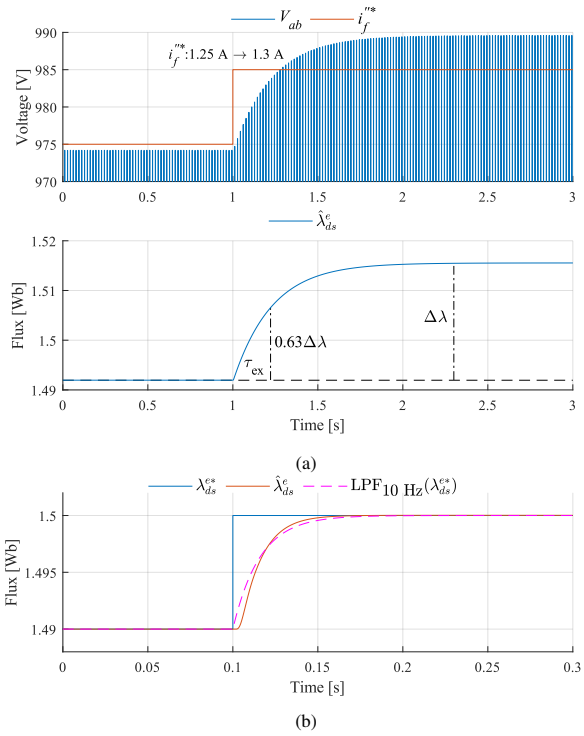

Fig. 3. Pretest results for (a) a parameter extraction and (b) a gain configuration of the stator flux regulator under the simulation.

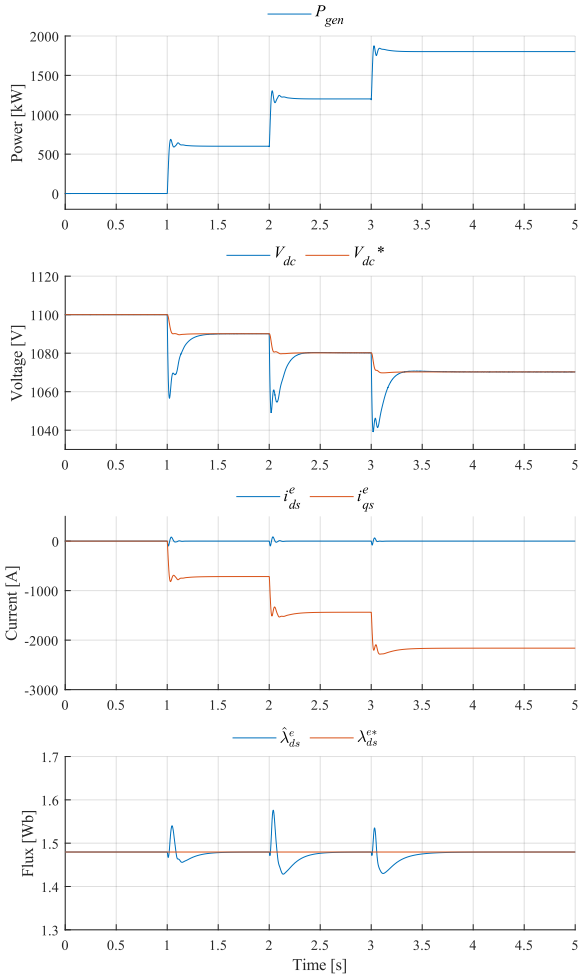

Fig. 4. Step response of the proposed SFOC under the simulation.

III. Simulation and Experimental Results

The proposed SFOC was implemented for a 1.8 MW WRSG and validated through simulation and experimental testing. The parameters of the test setup are shown in TABLE I. To determine the gains of the stator flux regulator, which had a target bandwidth of 10 Hz, a pretest was conducted. The pretest could be performed under the open terminal condition of the WRSG or zero current regulation of the AFE.

For the target system implemented in simulation, a pretest was conducted by varying $i_f''^*$ from 1.25 A to 1.3 A. The parameters were extracted through small signal analysis of the step response, as shown in Fig.3(a). By measuring the line voltage or utilizing the voltage set-point information of AFE, $\hat{\lambda}ds^e$ could be estimated. The time constant, τ_{ex}, of the transfer function from $i_f''^*$ to $\hat{\lambda}^e_{ds}$ was determined by observing the rise times to 63 % of the variation in $\hat{\lambda}^e_{ds}$. By inverting τ_{ex}, ω_{ex} was calculated as 4.5 rad/s. k_{ex} was calculated by dividing $\Delta\hat{\lambda}^e_{ds}$ by $\Delta i_f''^*$, resulting in a value of 0.48 Wb/A. Substituting the calculated parameters, ω_{ex} and k_{ex}, into (3) to achieve the target bandwidth by 10 Hz, the values of k_p and k_i were derived as 29 and 131, respectively.

Based on the calculated values of k_p and k_i, the stator flux regulator was implemented and assessed under set-point variation in a step-wise manner. Fig. 3 shows a comparison between the desired dynamic response and the step response of the flux regulator. The overlapped curves in the results indicate that the flux regulator achieved a control bandwidth of 10 Hz. The same process was repeated during the experiment to determine the appropriate values of k_p and k_i for the stator flux regulator.

The proposed SFOC was implemented based on the designed stator flux regulator and verified through tests with varying loads in a step-wise manner. Fig. 4 shows the step response with sequentially varying loads of 600 kW, 1200 kW, and 1800 kW. A droop configuration was applied, and the DC voltage setpoint was adjusted according to the generator's output power. Even under a step load change of 33% of the power ratings, the DC bus voltage converged within 0.3 s for all load variations. Furthermore, the stator flux, regulated by

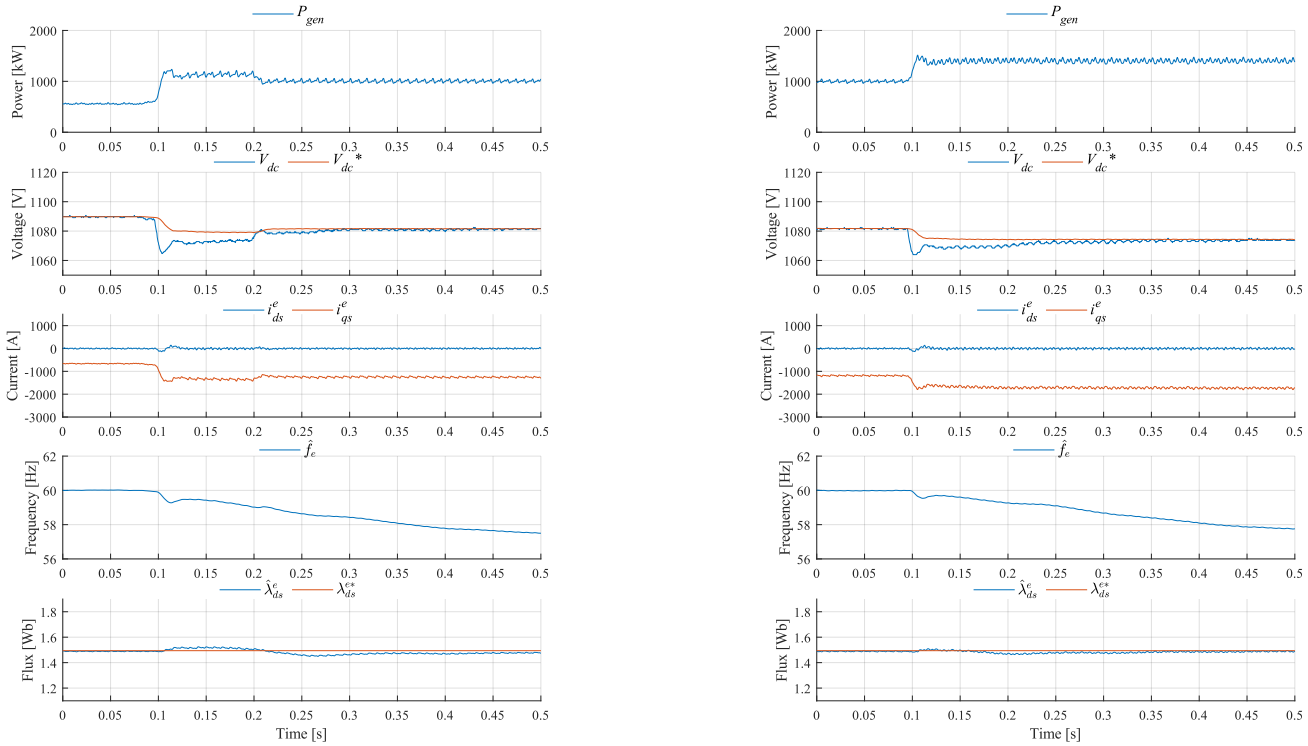

Fig. 5. Step response of the proposed SFOC, under load variation (a) from 550 kW to 1.05 kW, (b) and from 1050 kW to 1400 kW.

the finely tuned regulator, reached its setpoint within 0.5 s for all load variations.

Similarly, the proposed SFOC was verified through experiments with varying loads of 550 kW, 1050 kW, and 1400 kW. Fig. 5 shows the step response during the experiment. Although there was a frequency drop due to the slow dynamics of the governor, the DC bus voltage was regulated within 0.3 s, with voltage ripples of 2 V at steady state for all step load conditions. The estimated flux also converged to its setpoint within 0.2 s. Thanks to the consideration of the dynamics of the pilot exciter, the proposed SFOC demonstrated superior transient and steady-state performances.

IV. Conclusion

This paper proposed an SFOC method that takes into account the dynamics of the pilot exciter. By utilizing the approximated model of the pilot exciter, a flux regulator was designed in the form of a PI regulator to set the bandwidth of the flux regulation loop. Through simulation and experimental verification with a 1.8 MW WRSG, the proposed SFOC demonstrated flux regulation performance, achieving convergence within 0.5 s. Furthermore, the SFOC exhibited DC bus voltage regulation, achieving convergence within 0.3 s, as observed in both simulation and experimental tests.

References

[1] T.-H. Joung, S.-G. Kang, J.-K. Lee, and J. Ahn, "The imo initial strategy for reducing greenhouse gas (ghg) emissions, and its follow-up actions towards 2050," *Journal of International Maritime Safety, Environmental Affairs, and Shipping*, vol. 4, no. 1, pp. 1–7, 2020.

[2] T. C. Van, J. Ramirez, T. Rainey, Z. Ristovski, and R. J. Brown, "Global impacts of recent imo regulations on marine fuel oil refining processes and ship emissions," *Transportation Research Part D: Transport and Environment*, vol. 70, pp. 123–134, 2019.

[3] R. Geertsma, R. Negenborn, K. Visser, and J. Hopman, "Design and control of hybrid power and propulsion systems for smart ships: A review of developments," *Applied Energy*, vol. 194, pp. 30–54, 2017.

[4] J. Yun, Y.-K. Son, H.-J. Cho, and S.-K. Sul, "Dc bus voltage regulation strategy in maritime dc power system for minimized converter loss," *IEEE Transactions on Power Electronics*, vol. 36, no. 11, pp. 13 225–13 233, 2021.

[5] M. Imecs, C. Szabo, and I. I. Incze, "Stator-field-oriented vectorial control for vsi-fed wound-excited synchronous motor," in *2007 International Aegean Conference on Electrical Machines and Power Electronics*. IEEE, 2007, pp. 303–308.

[6] M. Imecs, I. I. Incze, and C. Szabo, "Stator-field oriented control of the synchronous generator: Numerical simulation," in *2008 International Conference on Intelligent Engineering Systems*. IEEE, 2008, pp. 93–98.

[7] A. K. Jain and V. Ranganathan, "Modeling and field oriented control of salient pole wound field synchronous machine in stator flux coordinates," *IEEE Transactions on Industrial Electronics*, vol. 58, no. 3, pp. 960–970, 2010.

[8] K. Satpathi, A. Ukil, J. Pou, and M. A. Zagrodnik, "Design, analysis, and comparison of automatic flux regulator with automatic voltage regulator-based generation system for dc marine vessels," *IEEE Transactions on Transportation Electrification*, vol. 4, no. 3, pp. 694–706, 2018.